Carbohydrate Polymers 84 (2011) 343–350

Contents lists available at ScienceDirect

Carbohydrate Polymers

journal homepage: www.elsevier.com/locate/carbpol

Thermoplastic starch–silica–polyvinyl alcohol composites by reactive extrusion

Kris Frost[a,*], Julien Barthes[a], Daniel Kaminski[a], Edmond Lascaris[b], Julie Niere[a], Robert Shanks[a]

[a] *CRC for Polymers, School of Applied Sciences, RMIT University, Australia*
[b] *Plantic Technologies Pty Ltd., Australia*

ARTICLE INFO

Article history:
Received 27 August 2010
Received in revised form 4 November 2010
Accepted 19 November 2010
Available online 25 November 2010

Keywords:
Thermoplastic starch
Silica
Composite
Reactive extrusion

ABSTRACT

Thermoplastic starch–silica (SiO_2) PVOH composite films were created via a reactive extrusion process using tetraethyl orthosilicate (TEOS) as a precursor. Reaction efficiency was determined by X-ray fluorescence measurement of film Si content and was observed to improve with increasing TEOS concentration. Films with high SiO_2 content were noted to have varying morphology and some SiO_2 clusters. Mechanical properties of the starch composite films were enhanced by even a small amount of SiO_2. Tensile strength and Young's modulus increased, while elongation at break decreased with increasing SiO_2 content. Dynamic mechanical analysis results showed that the starch–silica composite storage modulus increased and the loss modulus decreased with increasing SiO_2 content.

1. Introduction

Starch based thermoplastics are used in a range of film, film and packaging applications ranging from chocolate trays to agricultural coverings. Thermoplastic starch materials can be made from starch and chemically modified starch (De Graaf, Karman, & Janssen, 2003; Myllarinen, Buleon, Lahtinen, & Forssell, 2002; Rindlav-Westling, Stading, Hermansson, & Gatenholm, 1998; Yu, Dean, & Li, 2006).

Chemically modified starches are used in film production to inhibit retrogradation. Retrogradation is one of the causes of staling in breads and starch based foods, and involves the slow re-coiling of gelatinized amylose and amylopectin molecules back into their native helical arrangements or into a new, single helix conformation, the so called 'V' type structure (Gudmundsson, 1994).

Retrogradation in thermoplastic starch materials is undesirable as it imparts brittleness and a loss of optical clarity (Karim, Norziah, & Seow, 2000). A common chemically modified starch is hydroxypropylated starch. Hydroxypropylated starches are created through reaction with propylene oxide, which substitutes hydroxypropyl groups onto starch hydroxyls (De Graaf & Janssen, 2002). Hydroxypropylated starch produces thermoplastic films that are more flexible (Lafargue, Buléon, Doublier, & Lourdin, 2007). Poly(vinyl alcohol) (PVOH) can be readily blended with a hydroxypropylated starch, and starch PVOH blends have been proven to have better tensile strength and elongation than pure starch films (Lu, Xiao, & Xu, 2009), and the blend ratio and PVOH molecular weight can be adjusted to create desired mechanical properties (Fishman & Coffin, 2006; Mao, Imam, Gordon, Cinelli, & Chiellini, 2000).

Mechanical properties of polymers can also be altered by dispersing a second phase (e.g. fibers or particulates) through a primary phase. Composites with a nano-sized second phase show enhanced performance even at low filler volume fractions (Wetzel, Haupert, Friedrich, Zhang, & Rong, 2004).

The most common nano-fillers used to enhance mechanical properties in starch films are layered silicates or clays. These provide enhanced mechanical strength at low volume fractions provided that the nano-filler is well dispersed (Ray & Bousmina, 2005).

Another common nano-filler is silicon dioxide (silica or SiO_2). Shangwen Tang et al. reported that inclusion of dry powdered SiO_2 particles in starch–PVOH films increased tensile strength at break and improved water barrier properties (Tang, Xiong, & Tang, 2008). HanGuo Xiong et al. reported improved mechanical properties, transmittance, and water resistance of starch films containing nano-SiO_2 particles (Xiong, Tang, & Zou, 2008). Dispersion and mixing of silica particles requires high shear or ultrasonic mixing and nano-SiO_2 starch experiments have only been reported on a laboratory scale, typically by casting films from solution (Tang, Zou, et al., 2008; Wu, Wang, & Ge, 2009).

Silica particles can be prepared *in situ* within a hydrophilic polymer such as starch by the hydrolysis and condensation of alkoxysilanes in a mixture of water, alcohol and base catalyst. The most commonly used alkoxysilane is tetraethyl orthosilicate (TEOS). Because water and alkoxysilanes are generally immiscible, a mutual alcohol solvent such as ethanol is normally used to com-

---

* Corresponding author at: School of Applied Sciences, RMIT University, GPO Box 2476, Melbourne 3001, Australia. Tel.: +61 411 337 699.
E-mail address: frost.kris@gmail.com (K. Frost).

0144-8617/$ – see front matter. Crown Copyright © 2010 Published by Elsevier Ltd. All rights reserved.
doi:10.1016/j.carbpol.2010.11.042

patibilise the two (Klein, 1985). The choice of alcohol can have an effect on silica morphology. Silica particle size has been shown to increase with increasing molecular weight of the alcohol solvent; ethanol remains the preferred co-solvent due to small flocculation particle size and reduced silicon dioxide aggregate size after drying (Harris, Brunson, & Byers, 1990).

Alkoxysilane hydrolysis occurs by a nucleophilic mechanism. In basic conditions, water dissociates to produce hydroxide ions, which then attack the silicon atom. When the hydroxyl groups replace an alkoxyl group, the electron density of silicon is reduced, accelerating the hydrolysis rate of the other attached alkoxyl groups (Schmidt, Scholze, & Kaiser, 1984). Thus the rate limiting step in the reaction is hydrolysis of the first alkoxyl group, after which the hydrolysis proceeds rapidly producing silicic acid ($Si(OH)_4$) (Matsoukas & Gulair, 1988; Matsoukas & Gulari, 1989). After water is removed, the silicic acid condenses into silicon dioxide (SiO_2). The overall reaction can be written as:

$$Si(OR)_4 + 4H_2O \rightarrow Si(OH)_4 + 4ROH$$

$$nSi(OH)_4 \rightarrow nSiO_2 + 2nH_2O$$

Though the reaction of TEOS to SiO_2 appears simple, catalyst choice and concentration will vary SiO_2 morphology (Fuchigami, Taguchi, & Tanaka, 2008). The kinetics of TEOS to SiO_2 conversion has been widely studied, with resulting kinetic constants varying from author to author (Bailey & Mecartney, 1992; Bogush & Zukoski, 1991; Harris et al., 1990). Acid catalysis is much faster than base catalysis (Nagao et al., 2004). TEOS condensation reactions can form either large branched silica networks or small silicate particles depending on whether an acid or a base catalyst is used (Brinker, 1988).

Under base-catalysed conditions, the amount of silica formed is less than the amount of TEOS consumed, due to incomplete conversion of intermediate species such as silicic acid. Base-catalysed silica condensation is believed to involve the attack of a nucleophilic (de-protonated) silanol on a neutral silicic acid, thus agglomerate formation is dependent on silanol/silicic acid molecules being within close spacial proximity (Chen, Dong, Yang, & Yang, 1996). Base-catalysed TEOS condensation creates spherical silica agglomerates which impart different mechanical properties to the matrix into which they are incorporated.

The use of TEOS as a precursor to SiO_2 has enhanced mechanical properties in many different polymers, including poly(acrylonitrile-co-butadiene-co-styrene) (ABS), poly(butylene terephthalate) (PBT), poly(ethylene) (PE), poly(methyl methacrylate) (PMMA), poly(styrene-co-butadiene) rubber and poly(tetrafluroethylene) (PTFE, Teflon) (Barus, Zanetti, Lazzari, & Costa, 2009; Chen, Tsai, & Lee, 2004; Chinthamanipeta, Kobukata, Nakata, & Shipp, 2008; Gauthier, Reynauda, Vassoillea, & Ladouce-Stelandre, 2004; Hsu & Lin, 2000; Jiang et al., 2008).

SiO_2 can be incorporated into starch as a dry powder, or formed from TEOS via the sol–gel process then mixed into a starch slurry, and then solution cast. Alternatively thermoplastic starch composites with SiO_2 may be produced via reactive extrusion. Reactive extrusion has been used to produce hydroxypropylated starch, starch succinates, carboxylic acid modified starches and starch phosphates (Carvalho, Zambon, da Silva Curvelo, & Gandini, 2005; De Graaf & Janssen, 2002; O'Brien, Wang, Vervaet, & Remon, 2009; Wang, Shogren, & Willett, 1997).

TEOS, hydroxypropylated starch, PVOH and a base catalyst (NH_3) were combined in a reactive extrusion process to investigate film mechanical properties of starch–silica PVOH composites.

Table 1
Axon B12 extruder temperature zone settings (°C).

Zone 1	Zone 2	Zone 3	Zone 4
60	90	80	70

2. Materials and methods

Eco Film™, a high amylose (80%), hydroxypropylated starch (DS 0.17) was supplied by National Starch (US). PVOH (Elvanol 71-30) was supplied by DuPont Australia. TEOS and catalysts were purchased through Sigma Aldrich.

2.1. Preparation of materials using single screw extrusion

Starch batches (300 g) were prepared containing 3.5% (w/w) of TEOS, 10% (w/w) ethanol, 10%(w/w) PVOH and slurried using 310 ml of water. Ammonia, hydrochloric acid and sodium hydroxide were added as catalysts at 0.001, 0.01, 0.1 and 1 M in the starch slurry. The control was also made to a total mass of 300 g incorporating 10% (w/w) PVOH, 3.5% (w/w) TEOS and slurried with 330 ml of water. The slurries were then extruded using an Axon B-12 single screw extruder producing a single 6 mm strand which was pelletised. Films were formed through the hot-pressing of pellets using 20 tons of pressure at 120 °C for 5 min. Table 1 displays the Axon B-12 extruder settings.

2.2. Preparation of materials using twin screw extruder

Film was prepared on a twin screw, co-rotating Entek 27 extruder. TEOS, ammonia [0.01 M], water and ethanol were added as a liquid feed (6.1 kg/h). Solid powders were added at 9.1 kg/h. Ethanol concentration in both the single screw and twin screw reactive extrusion experiments was fixed at 10% (w/w), as this was deemed the maximum safe concentration allowable in an extrusion environment by and independent occupational health and safety risk assessment. For experimental simplification, TEOS was added in amounts to create approximate silica dioxide film contents of 0, 0.5, 1, 1.5, 2, 2.5 and 3% (w/w) based on the assumption of 100% conversion of TEOS to SiO_2 (Table 2). While 100% conversion has low probability, the exact conversion rates in a reactive extrusion environment are not known and could not be readily estimated.

Sheets were extruded using a 620 mm die at a gauge of 250 μm and collected on roll stacks at 80 °C. Sheets were then left to equilibrate at 23 °C and 50% relative humidity prior to mechanical testing. Table 3 details the Entek 27 parameters used.

2.3. Determination of film SiO_2 content by X-ray fluorescence analysis

A Bruker S4 Pioneer wavelength dispersive X-ray fluorescence spectrometer was used to determine actual SiO_2 content in the films. Calibration standards were prepared by addition of pure dry SiO_2 to dried starch, which was then re-hydrated and hot pressed into films of 200, 300 and 600 μm thickness. Calibration equations did not change with regard to thickness; for silica in graphite, 90% of the radiation will originate from within 48.9 μm of the surface (Scholtz & Uhlig, 2002).

2.4. Stress–strain analysis

Stress–strain testing was conducted on an Instron™ 4465 materials tester using a 5 kN load cell. Samples were tested according to ASTM D638 using type IV test specimen standards. A strain rate of 2 mm/min was used.

Table 2
Formulations for thermoplastic starch–silica composites.

Film designation	EcoFilm starch (w%)	Elvanol 71-30 PVOH (w%)	Stearic acid (w%)	Ethanol (w%)	TEOS (w%)	Water (w%)
0% SiO_2	66.1	7.6	0.1	7.3	0	18.9
0.5% SiO_2	65.7	7.6	0.1	7.3	0.4	18.9
1% SiO_2	65.4	7.6	0.1	7.3	0.7	18.9
1.5% SiO_2	65.0	7.6	0.1	7.3	1.1	18.9
2% SiO_2	64.6	7.6	0.1	7.3	1.5	18.9
2.5% SiO_2	64.3	7.6	0.1	7.3	1.8	18.9
3% SiO_2	63.9	7.6	0.1	7.3	2.2	18.9

2.5. *Dynamic mechanical testing*

Storage and loss modulus for starch materials were measured using a Perkin Elmer Diamond DMA at a constant temperature of 25 °C with an applied frequency of 1 Hz, and results averaged over five replicates.

2.6. *Film morphology using environmental scanning electron microscopy (ESEM)*

Film SiO_2 morphologies were examined using a FEI Quanta 200 environmental scanning electron microscopy (ESEM) with EDAX Si(Li) X-ray detector. Presence of Si in films was confirmed using the ESEM EDAX attachment. A high vacuum was used along with a generator setting of 30 kV and spot size of 3. Use of generator settings above 30 kV caused sample degradation to occur before a high resolution image could be obtained. Films were lightly etched in 1 M HCl and dried before analysis.

3. Results and discussion

3.1. *Films produced using single screw extrusion*

To examine the effects of catalyst choice and concentration on starch–PVOH film morphology, and to determine an optimum catalyst concentration for twin screw extrusion, starch composite films were prepared using a fixed concentration of TEOS, PVOH and ethanol, with varying acid and base concentrations. For experimental simplicity TEOS concentration was initially fixed at 3.5%, under the assumption that the full conversion of 3.5% (w/w) TEOS (M_r 208.33) to SiO_2 (M_r 60.09) would yield approximately 1% (w/w) SiO_2 film content. The *in situ* creation of SiO_2 in starch–PVOH films within the range of 0–3% (w/w) was considered achievable for larger scale twin screw extrusion. Previous literature on starch–silica PVOH composites also suggests that a morphological and mechanical optimum in found between 1 and 3% (w/w) SiO_2 film content (Tang, Xiong, et al., 2008; Tang, Zou, et al., 2008; Wu et al., 2009).

Table 3
Entek 27 extrusion parameters.

Parameter	Set value
Screw speed	300 RPM
Zone 1 temp	40 °C
Zone 2 temp	70 °C
Zone 3 temp	80 °C
Zone 4 temp	90 °C
Zone 5 temp	95 °C
Zone 6 temp	120 °C
Zone 7 temp	135 °C
Zone 8 temp	135 °C
Zone 9 temp	130 °C
Zone 10 temp	120 °C
Zone 11 temp	110 °C
Zone 12 temp	90 °C
Die Zone 1 temp	110 °C
Die Zone 2 temp	120 °C
Die Zone 3 temp	120 °C
Die Zone 4 temp	110 °C

Image 1a through to Image 1i display the examples of morphologies found in samples produced using the Axon B12 extruder with a fixed content of 3.5% (w/w) TEOS and varying types and concentrations of catalyst.

Acidic (HCl) conditions produced needle like SiO_2 crystals (Image 1a and b) whereas basic conditions produced spherical SiO_2 agglomerates (Image 1d, e, f, h and i). After one week, acid-catalysed films stored at 23 °C and 50% RH began to degrade due to acid hydrolysis of starch (Image 1c). Sodium hydroxide catalysis turned films brown. The brown taint was noted to deepen in colour with increasing sodium hydroxide concentration. Ammonia catalysed films did not display any browning. Low concentrations of basic catalysts (0.001 M) did not increase the natural pH of starch slurries above pH 7 and a variety of morphologies was observed in these films, ranging from spherelites to needles and chain growth (see Image 1g). Base-catalysed SiO_2 agglomerates ranged from 20 microns to <1 micron in diameter and were evenly distributed. The effect of catalyst concentrations above 0.01 M had no further effect on agglomerate morphology.

Films prepared without ethanol produced fewer SiO_2 particles (Image 1f). Ammonia (at or above 0.01 M) was selected as the optimal catalyst because it did not cause film browning, produced similar SiO_2 morphology to NaOH catalysed films and did not show signs of film degradation at up to 8 weeks when stored at 23 °C and 50% RH.

3.2. *Films produced using twin screw extrusion*

Extruded starch molecules, like many semi-crystalline polymers, preferentially align in the direction of extrusion flow (Kaito, Kyotani, & Nakayama, 2003; Laun, 1984; Lindenmeyer & Lustig, 2003) and thus the transverse direction of the films tends to have poorer elongation (Honeker & Thomas, 1996; Imada, Yamamoto, Shigematsu, & Takayanagi, 1971; Zhou & Wilkes, 1998). Due to this extrusion effect the starch–PVOH control produced using an Entek 27 twin screw extruder displayed a higher elongation and lower modulus and tensile strength in the machine direction compared to the transverse direction.

Starch–silica PVOH composite films were prepared on an Entek 27 twin screw extruder using ammonia (0.01 M) as a catalyst, previously determined as the optimum choice, and varying concentrations of TEOS. Table 4 displays the reaction efficiency results of SiO_2 formation versus TEOS addition. The conversion efficiency of TEOS to SiO_2 varied from 12.0 to 41.3%. The highest efficiency (41.3%) was obtained with the highest addition amount of TEOS and a target SiO_2 of 3% (w/w). The short reaction time during the extrusion process (approximately 3 min) may have reduced the yield of SiO_2.

SiO_2 particles were spherical and formed agglomerates between 20 μm and <1 μm in diameter, particles <0.5 μm could not be observed due to the resolution limitations of the ESEM. Films with high TEOS content showed large-scale SiO_2 clustering. Image

Table 4
TEOS to SiO_2 conversion efficiency.

Desired SiO_2% (w/w)	TEOS (g)	Desired SiO_2 (g) in 10 kg	SiO_2 (g) produced in 10 kg starch	Actual SiO_2% (w/w)	Efficiency %
0.50	173.3	50	6.0	0.06	12.0
1.00	346.7	100	12.0	0.12	12.0
1.50	520.0	150	21.5	0.22	14.3
2.00	693.3	200	28.5	0.29	14.3
2.50	866.7	250	58.5	0.59	23.4
3.00	1040.0	300	124.0	1.24	41.3

2a shows typical SiO_2 dispersion and agglomerate size observed throughout all films. Image 2b shows the presence of large clusters (>50 μm) in films prepared using the highest TEOS concentration.

3.3. Mechanical property analysis

Fig. 1 shows elongation at break and elongation at yield in machine and transverse directions for the various SiO_2 concentrations ranging from 0 to 1.25% (w/w). Elongation at break decreased as SiO_2 content increased, while elongation at yield remained relatively constant.

Film ultimate and yield stress rose quickly with increasing SiO_2 content, Fig. 2 displays the logarithmic relationship observed between SiO_2 content and tensile properties. At 1% (w/w) SiO_2 inclusion machine and transverse tensile strength increased by 65% with respect to the control. The observed logarithmic trends and

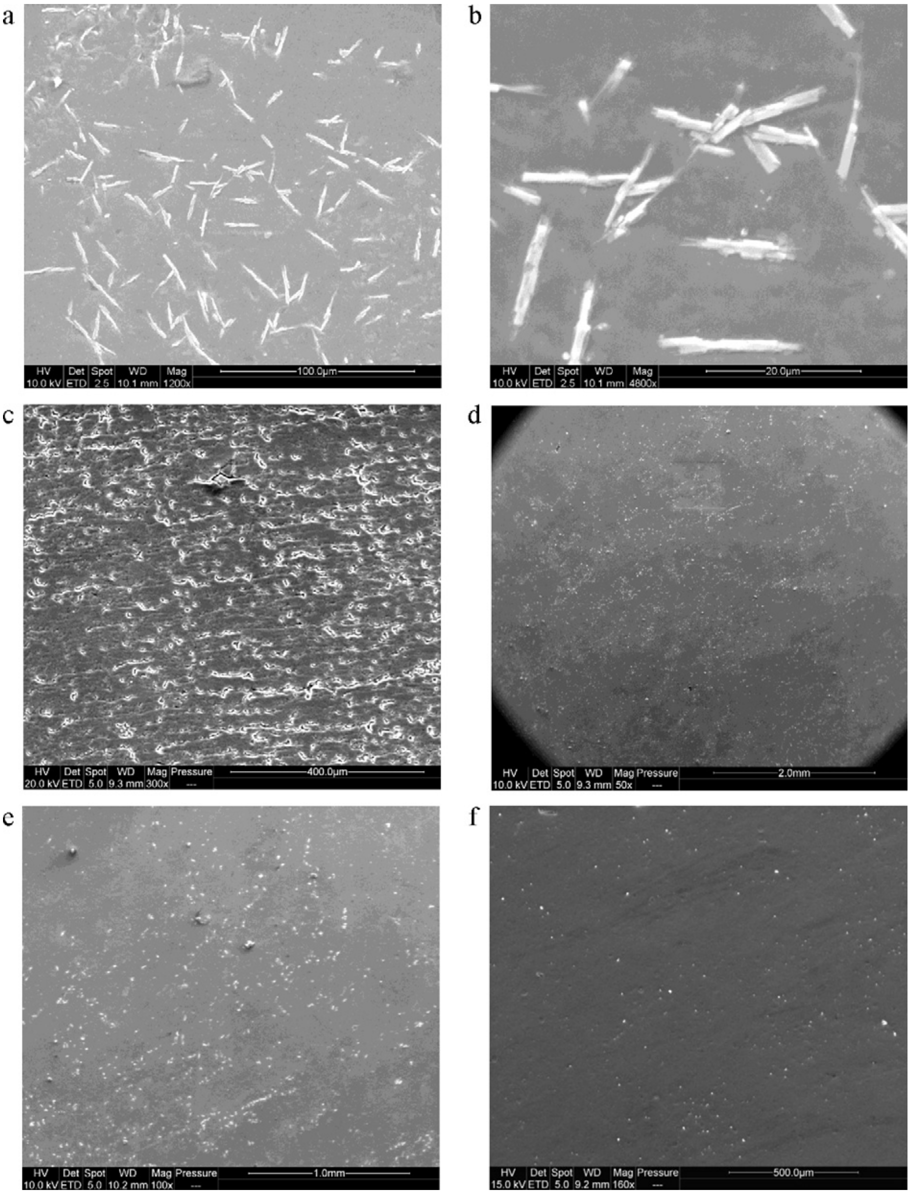

Image 1. (a) SiO_2 crystals formed in HCl catalysed (0.1 M) films. (b) Higher magnification of image 1a. (c) Degraded film (0.1 M HCl) with holes after one month due to acid hydrolysis. (d) SiO_2 spherelites and agglomerates formed in NaOH catalysed (0.1 M) films. (e) Higher magnification of SiO_2 particles in NaOH catalysed (0.1 M) films. (f) SiO_2 morphology in NaOH catalysed (0.1 M) films with no ethanol. (g) Silica chain growth observed in low (0.001 M) NH_3 catalysed film. (h) SiO_2 particle size and distribution in NH_3 (0.1 M) catalysed films. (i) Higher magnification of SiO_2 agglomerates in NH_3 catalysed (0.1 M) films.

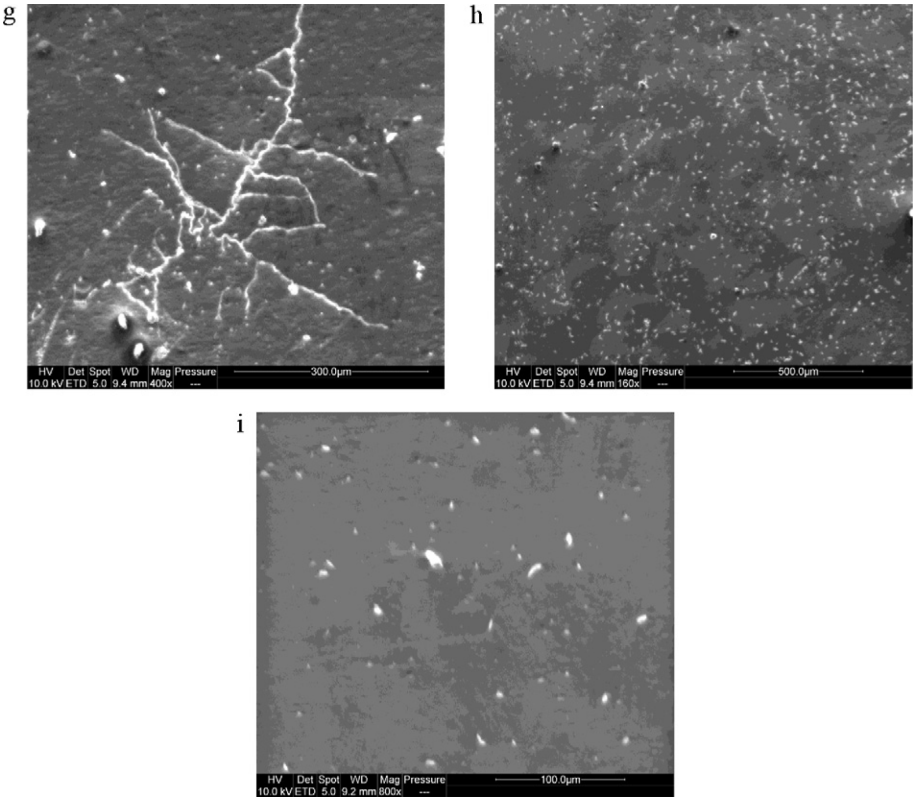

Image 1. (*Continued*)

increase in tensile strength were similar to results reported by Tang, Zou, et al. (2008).

Young's modulus of the films also increased with addition of SiO_2, in both the machine and transverse directions. The relationship between SiO_2 content and film modulus was also observed to be logarithmic (Fig. 3). At 1% (w/w) SiO_2, film transverse modulus was 350 MPa greater than the control, and the machine modulus was 110 MPa greater.

3.4. Dynamic mechanical analysis (DMA)

Similar to mechanical testing results, DMA storage modulus and loss modulus displayed logarithmic trends (Fig. 4). As silica content increased the films were able to store more energy resulting in a decreased elastic response to applied forces, as indicated by the increase in storage modulus. The loss modulus values show that the films lose the ability to efficiently disperse energy with increasing SiO_2 concentration. Silica reacts with starch to form starch–silica ethers, and this covalent bonding coupled with subsequent mild physical cross-linking effects increased overall tensile strength and reduced elongation.

Mechanical properties of the starch–silica PVOH composites changed with even small amounts (0.25%, w/w) of *in situ* formed SiO_2. Due to extrusion induced starch and PVOH molecular alignment in films, SiO_2 formation effected mechanical properties in the machine and transverse direction in an un-homogeneous manner. Reactive extrusion of TEOS using a base catalyst in a starch PVOH blend produced films with small, well dispersed SiO_2 agglomerates. These agglomerates have a high surface area and can interact with

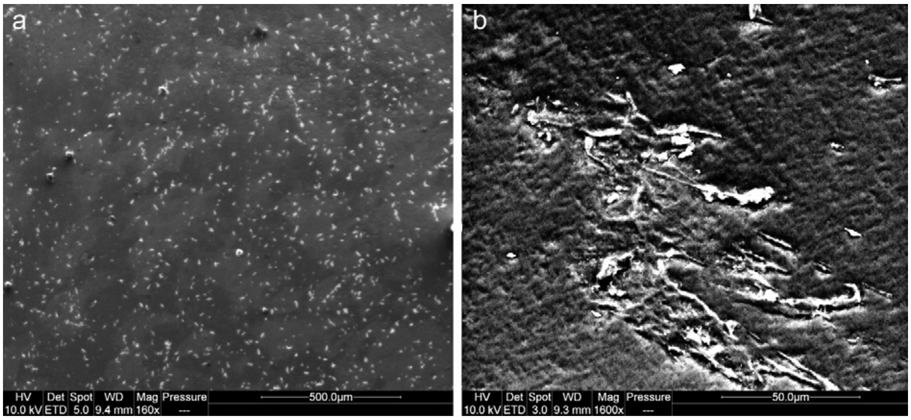

Image 2. (a) ESEM of film containing 0.59% w/w SiO_2 (b) clustering observed in film containing 1.24% w/w SiO_2.

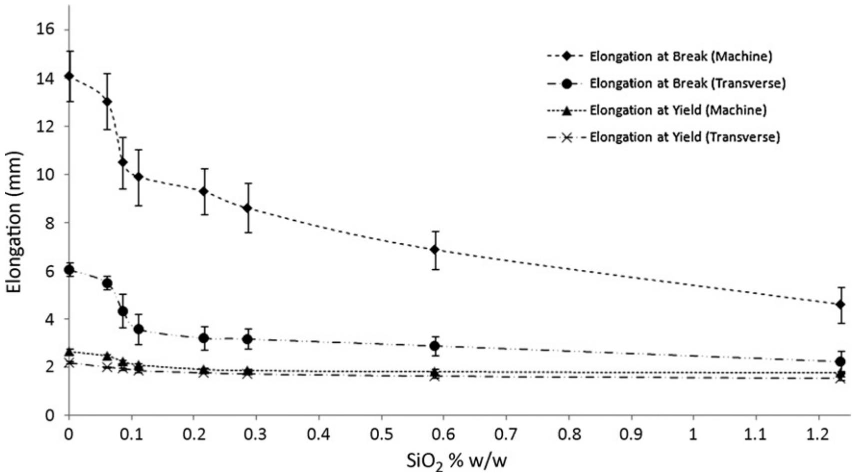

Fig. 1. Elongation at break and yield in machine and transverse directions (including standard error) versus SiO_2 content.

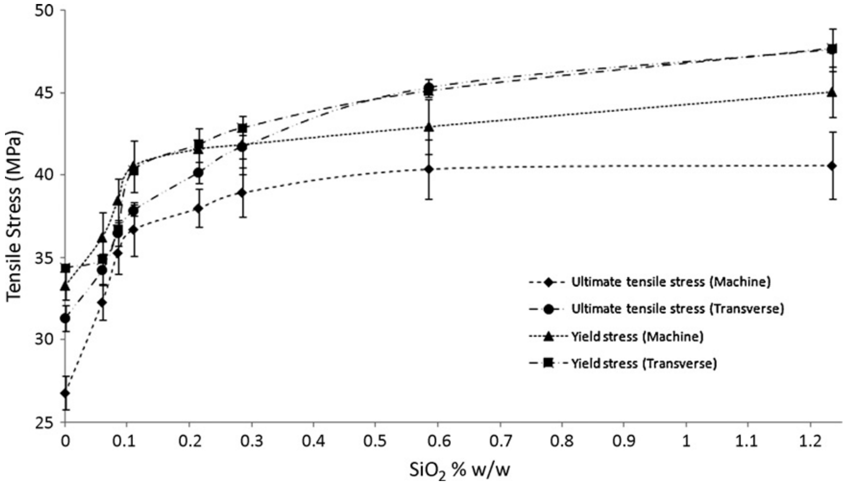

Fig. 2. Ultimate tensile stress and stress at yield in machine and transverse film directions (including standard error) versus SiO_2 content.

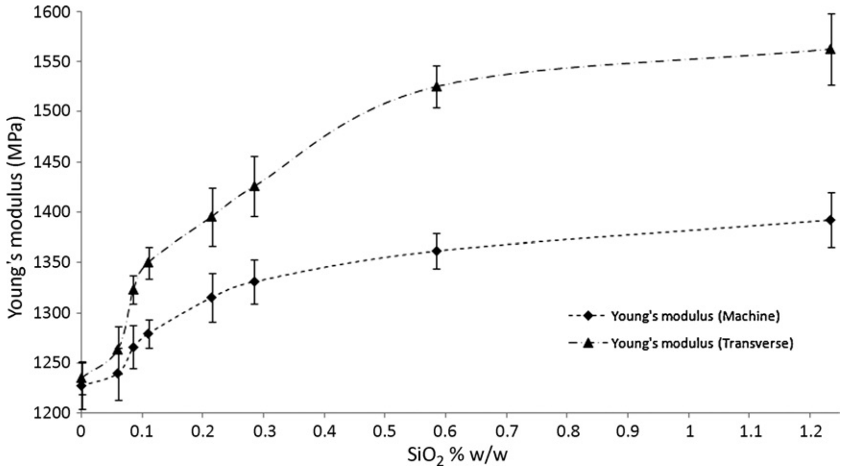

Fig. 3. Young's modulus (MPa) in both machine and transverse film directions (including standard error) versus SiO_2 content.

starch and PVOH through hydrogen bonding and ether formation. A small increase in the volume fraction of film SiO_2 rapidly affected mechanical properties by reducing starch and PVOH molecular slip, decreasing elongation and visco-elastic response, but enhancing Young's modulus and tensile strength.

4. Conclusion

The reactive extrusion of hydroxypropylated starch, TEOS, PVOH, ethanol and catalyst successfully created films with small, well dispersed SiO_2 agglomerates. During twin screw extrusion TEOS to SiO_2 conversion efficiencies of up to 41.3% were achieved.

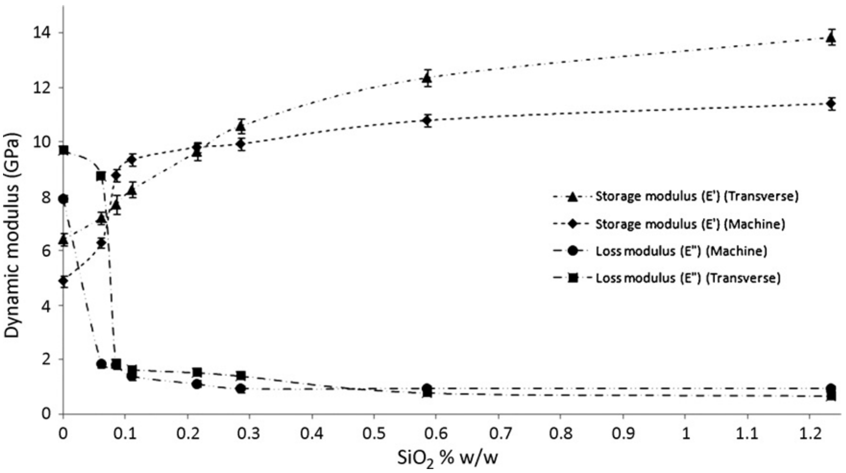

Fig. 4. DMA results showing storage modulus and loss modulus in machine and transverse film directions (including standard error) versus SiO_2 content.

SiO_2 film morphology was dependant on catalyst and ethanol inclusion. Acid catalysis (HCl) produced needle like SiO_2 aggregates and base catalysis (NH_3 and NaOH) produced spherical agglomerates. SiO_2 particle size ranged from 20 μm to <1 μm. The optimum catalyst concentration in both acid and base reactions was determined to be approximately 0.01 M. The addition of base catalyst at concentrations above 0.01 M produced no extra effect on SiO_2 morphology or distribution. Without ethanol as a co-solvent the observable SiO_2 agglomerate population was reduced.

The starch–silica PVOH composites had a higher tensile strength in comparison to a control, but a lower elongation at break. Tensile strength increased by 65% with 1% (w/w) SiO_2 and elongation at break decreased by 69%. SiO_2 agglomerates can hydrogen bond or form ethers with surrounding starch and PVOH molecules, rapidly reducing elongation and enhancing modulus and tensile strength.

This was the first reported reactive extrusion of a starch–silica PVOH composite film using TEOS as a SiO_2 precursor. Although reaction efficiencies were low, optimization was not an objective. A small inclusion of well dispersed SiO_2 was observed to have a large effect on film mechanical properties.

References

Bailey, J. K., & Mecartney, M. L. (1992). Formation of colloidal silica particles from alkoxides. *Colloids and Surfaces*, *63*, 151–161.

Barus, S., Zanetti, M., Lazzari, M., & Costa, L. (2009). Preparation of polymeric hybrid nanocomposites based on PE and nanosilica. *Polymer*, *50*, 2595–2600.

Bogush, G. H., & Zukoski, I. V. C. F. (1991). Studies of the kinetics of the precipitation of uniform silica particles through the hydrolysis and condensation of silicon alkoxides. *Colloid and Interface Science*, *142*(1), 1–18.

Brinker, C. J. (1988). Hydrolysis and condensation of silicates: effects on structure. *Non-Crystalline Solids*, *100*, 31–50.

Carvalho, A. J. F., Zambon, M. D., da Silva Curvelo, A. A., & Gandini, A. (2005). Thermoplastic starch modification during melt processing: Hydrolysis catalyzed by carboxylic acids. *Carbohydrate Polymers*, *62*, 387–390.

Chen, S., Dong, P., Yang, G., & Yang, J. (1996). Kinetics of formation of monodisperse colloidal silica particles through the hydrolysis and condensation of tetraethylorthosilicate. *Industrial Engineering Chemistry*, *35*, 4487–4493.

Chen, Y., Tsai, C., & Lee, Y. (2004). Preparation and properties of silylated PTFE/SiO_2 organic-inorganic hybrids via sol–gel process. *Polymer Science: Part A*, *42*(7), 1789–1807.

Chinthamanipeta, P. S., Kobukata, S., Nakata, H., & Shipp, D. A. (2008). Synthesis of poly(methyl methacrylate)–silica nanocomposites using methacrylate-functionalized silica nanoparticles and RAFT polymerization. *Polymer*, *49*, 5636–5642.

De Graaf, R. A., & Janssen, L. P. B. M. (2002). The hydroxypropylation of starch in a self-wiping twin screw extruder. *Advances in Polymer Technology*, *22*(1), 56–68.

De Graaf, R. A., Karman, A. P., & Janssen, L. P. B. M. (2003). Material properties and glass transition temperatures of different thermoplastic starches after extrusion processing. *Starch-Starke*, *55*(2), 80–86.

Fishman, M. L., & Coffin, D. R. (2006). Two stage extrusion of plasticized pectin/poly(vinyl alcohol) blends. *Carbohydrate Polymers*, *65*, 421–429.

Fuchigami, K., Taguchi, Y., & Tanaka, M. (2008). Synthesis of spherical silica particles by sol–gel method and application. *Polmers for Advanced Technologies*, *19*, 977–983.

Gauthier, C., Reynauda, E., Vassoillea, R., & Ladouce-Stelandre, L. (2004). Analysis of the non-linear viscoelastic behaviour of silica filled styrene butadiene rubber. *Polymer*, *45*, 2761–2771.

Gudmundsson, M. (1994). Retrogradation of starch and the role of its components. *Thermochimica Acta*, *246*, 329–341.

Harris, M. T., Brunson, R. R., & Byers, C. H. (1990). The base catalyzed hydrolysis and condensation reactions of dilute and concentrated TEOS solutions. *Non-Crystalline Solids*, *121*, 397–403.

Honeker, C., & Thomas, E. L. (1996). Impact of morphological orientation in determining mechanical properties in triblock copolymer systems. *Chemistry of Materials*, *8*(8), 1702–1714.

Hsu, Y. G., & Lin, F. J. (2000). Organic–inorganic composite materials from acrylonitrile–butadiene–styrene copolymers (ABS) and silica through an in situ sol–gel process. *Applied Polymer Science*, *75*, 275–283.

Imada, K., Yamamoto, T., Shigematsu, K., & Takayanagi, M. (1971). Crystal orientation and some properties of solid-state extrudate of linear polyethylene. *Materials Science*, *6*(6), 537–546.

Jiang, Z., Siengchin, S., Zhou, L., Steeg, M., Karger-Kocsis, J., & Man, H. C. (2008). Poly (butylene terephthalate)/silica nanocomposites prepared from cyclic butylene terephthalate. *Composites: Part A*, *40*(3), 273–278.

Kaito, A., Kyotani, M., & Nakayama, K. (2003). Effects of shear rate on the molecular orientation in extruded rods of a thermotropic liquid crystalline polymer. *Applied Polymer Science*, *55*(10), 1489–1493.

Karim, A. A., Norziah, M. H., & Seow, C. C. (2000). Methods for the study of starch retrogradation. *Food Chemistry*, *71*, 9–36.

Klein, L. C. (1985). Sol–gel processing of silicates. *Annual Revision Material Sciences*, *15*, 227–248.

Lafargue, D., Buléon, P. B., Doublier, A., & Lourdin, J. LD. (2007). Structure and mechanical properties of hydroxypropylated starch films. *Biomacromolecules*, *8*, 3950–3958.

Laun, H. M. (1984). Orientation effects and rheology of short glass fiber-reinforced thermoplastics. *Colloid and Polymer Science*, *262*(4), 257–269.

Lindenmeyer, P. H., & Lustig, S. (2003). Crystallite orientation in extruded polyethylene film. *Applied Polymer Science*, *9*(1), 227–240.

Lu, D. R., Xiao, C. M., & Xu, S. J. (2009). Starch-based completely biodegradable polymer materials. *eXPRESS Polymer Letters*, *3*(6), 366–375.

Mao, L, Imam, S., Gordon, S., Cinelli, P., & Chiellini, E. (2000). Extruded corn starch–glycerol–polyvinyl alcohol blends: Mechanical properties, morphology and biodegradability. *Polymers and the Environment*, *8*(4), 205–211.

Matsoukas, T., & Gulair, E. (1988). Dynamics of growth of silica particles from ammonia-catalyzed hydrolysis of tetraethylorthosilicate. *Colloid and Interface Science*, *124*(1), 252–261.

Matsoukas, T., & Gulari, E. (1989). Monomer addition growth with a slow initiation step: a growth model for silica particles from alkoxides. *Colloid and Interface Science*, *132*(1), 13–21.

Myllarinen, P., Buleon, A., Lahtinen, R., & Forssell, P. (2002). The crystallinity of amylose and amylopectin films. *Carbohydrate Polymers*, *48*, 41–48.

Nagao, D., Osuzu, H., Yamada, A., Mine, E., Kobayashi, Y., & Konno, M. (2004). Particle formation in the hydrolysis of tetraethyl orthosilicate in pH buffer solution. *Colloid and Interface Science*, *279*, 143–149.

O'Brien, S., Wang, Y., Vervaet, C., & Remon, J. P. (2009). Starch phosphates prepared by reactive extrusion as a sustained release agent. *Carbohydrate Polymers*, *76*, 557–566.

Ray, S. S., & Bousmina, M. (2005). Biodegradable polymers and their layered silicate nano composites: In greening the 21st century materials world. *Progress in Materials Science*, *50*(8), 962–1079.

Rindlav-Westling, A., Stading, M., Hermansson, A. M., & Gatenholm, P. (1998). Structure, mechanical and barrier properties of amylose and amylopectin films. *Carbohydrate Polymers*, *36*, 217–224.

Schmidt, H., Scholze, H., & Kaiser, A. (1984). Principles of hydrolysis and condensation reaction of alkoxysilanes. *Non-Crystalline Solids*, *63*, 1–11.

Scholtz, R., & Uhlig, S. (2002). *Introduction to X-ray Fluorescence Analysis (XRF)*. Karlsruhe, Germany: Bruker AXS Gmbh.

Tang, S., Xiong, Z. P., & Tang, H. H. (2008). Effect of nano-SiO_2 on the performance of starch/polyvinyl alcohol blend films. *Carbohydrate Polymers*, *72*, 521–526.

Tang, S., Zou, P., Xiong, H., & Tang, H. (2008). Effect of nano-SiO_2 on the performance of starch/polyvinyl alcohol blend films. *Carbohydrate Polymers*, *72*, 521–526.

Wang, L., Shogren, R. L., & Willett, J. L. (1997). Preparation of starch succinates by reactive extrusion. *Starke*, *49*(3), 116–120.

Wetzel, B., Haupert, F., Friedrich, K., Zhang, M. Q., & Rong, M. Z. (2004). Impact and wear resistance of polymer nanocomposites at low filler content. *Polymer Engineering and Science*, *42*(9), 1919–1927.

Wu, M., Wang, M., & Ge, M. (2009). Investigation into the performance and mechanism of SiO_2 nanoparticles and starch composite films. *The Textile Institute*, *100*(3), 254–259.

Xiong, H., Tang, T. S., & Zou, P. (2008). The structure and properties of a starch-based biodegradable film. *Carbohydrate Polymers*, 263–268.

Yu, L., Dean, K., & Li, L. (2006). Polymer blends and composites from renewable resources. *Progress in Polymer Science*, *31*, 576–602.

Zhou, H., & Wilkes, G. L. (1998). Orientation-dependent mechanical properties and deformation morphologies for uniaxially melt-extruded high-density polyethylene films having an initial stacked lamellar texture. *Materials Science*, *33*(2), 287–303.